BLOCK MODELING OF PRESENT-DAY DEFORMATION OF ANATOLIA AND SLIP RATES ALONG THE NORTH ANATOLIAN FAULT

by

MEHMET KOKUM

Submitted to faculty of University Graduate School

in partial fulfillment of the requirements for the degree Master of Science

In the Department of Geological Science

Indiana University

July 2012

ProQuest LLC.
789 East Eisenhower Parkway
P.O. Box 1346
Ann Arbor, MI 48106 - 1346

Accepted by the Graduate Faculty, Indiana University in partial fulfillment of the requirements for the degree of Master of Science in Geological Sciences.

_____

Kaj M. Johnson, Chairman

_____

Michael W. Hamburger

_____

Gary L. Pavlis

Acknowledgements

I would like to thank my advisor, Dr. Kaj Johnson for his guidance throughout this research. His patience and intelligence are wonderful synthesis to be a great adviser. I feel so lucky to have chance to work under Dr. Kaj. Working with him was fun and it thought me a lot.

I would also like to thank Dr. Michael Hamburger for being always available and willing to help throughout my studies, as well as Dr. Gary Pavlis for help me to learn software to improve my research project. I would like to thank Ray Chung for patiently answering to my countless questions.

I would like to thank Republic of Turkey Ministry of National Education for financial support.

I also would like to thank to Ms. Mary Iverson for her help and patience throughout my attempts to graduate.

I also very appreciate to all members of my family for their love and prayers throughout this process.

Block Modeling of Present-Day Deformation of Anatolia and Slip Rates Along the North Anatolian Fault

By Mehmet Kokum

I use GPS velocity field and published geologic slip rates to constrain an elastic block model for Anatolia and surrounding regions. The elastic block model allows us to define plate motion and both strike and tensile slip rates along the major faults. Previous studies (eg., McClusky et al., 2000; Reilinger et al., 2006) have pointed to the discrepancy between geodetic-derived slip rate estimates of around 25 mm/yr on the North Anatolian Fault (NAF) and geologically-derived slip rate estimates of roughly 18 mm/yr. To address this discrepancy, I conduct two inversions; a geodetic-only inversion and a joint inversion. While I constrain one model with only geodetic data, I constrain the other model with both geodetic data and geologic slip rates. On the basis of the GPS velocity field, the Anatolia and Aegean blocks show counterclockwise motion with respect to the Eurasian plate, and the rate of this motion is increasing towards to the Hellenic arc. The geodetic-only inversion gives higher slip rate and deeper locking depth estimates for the North Anatolian Fault than joint inversion. The geodetic-only inversion gives a North Anatolian Fault (NAF) slip rate of approximately 26-27 mm/yr with locking depths of 20-25 km (preferably 23 km). The joint inversion gives a NAF slip rate of approximately 18-19 mm/yr with a shallower locking depths of 12-16 km (preferably 14 km). The geodetic-only inversion fits the GPS data better than the joint inversion with a normalized chi-square of 2.8-2.9 compared to the joint inversion normalized chi-square

value of 3.1-3.2. However, the slip rates in the joint inversion are consistent with the geologic slip rates and the locking depths of 12-16 km are consistent with the depth of background seismicity, suggesting this result is consistent with more observational constraints than the geodetic-only inversion.

Table of Contents

List of Figures

List of Tables

Chapter 1 - Tectonic Setting and Research Problem

A. Tectonic Setting

The main tectonic features of the Anatolian Plate are complicated by the collision between the Arabian and African plate in the south and Eurasian plate in the north and subduction of the African plate beneath the Anatolian plate along the Aegean-Cyprus arc. As a result of these complex tectonic structures, the Anatolian plate displays various tectonic styles simultaneously (Figure 1).

Tectonic plates are thought to be relatively rigid blocks of crust with deformation concentrated along plate boundaries in response to applied stress. Oceanic plate boundaries are represented by narrow and relatively simple deformation zones. Continental convergent plate boundaries are represented by broad, diffuse and more complex deformation zones, where the deformation extends up to thousands of kilometers (McKenzie, 1972).

Using epicenters and focal mechanisms of earthquakes, McKenzie (1970) defined the Turkish (Anatolian) and Aegean plates based on the observation that there exist different tectonic regimes in Turkey than those in its surrounding region. He claimed that Turkey and Greece are seismically much more active than that of western Mediterranean, and fault plane solutions are quite complicated. This difference is a consequence neither of the collision between Africa and Europe, nor result of the opening of the Red Sea. The basis of increasing activity in this area is the existence of two moving small plates; one is called Aegean Plate and includes the Aegean, part of western Turkey, part of Greece; the other one is called the Turkish or Anatolian Plate including most of Turkey and Cyprus.

McKenzie (1970) further suggested that Aegean plate is moving southwestwards with respect to Africa, resulting in the subduction of the African plate, while the Anatolian plate is moving west with respect to Europe and Africa along the North and East Anatolian faults.

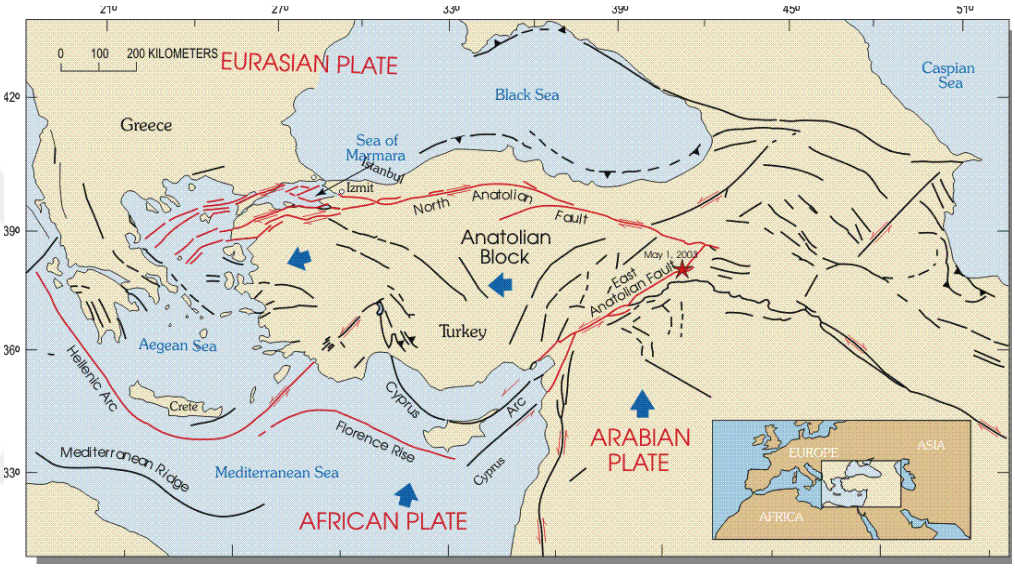

Figure 1. Main tectonic features of Anatolia from Implications for Earthquake Risk Reduction in the United States from the Kocaeli, Turkey, Earthquake of August 17, 1999.

Bozkurt (2001) emphasized that there are three main neotectonic structures in Turkey: (1) the North and (2) East Anatolian faults and (3) the Aegean-Cyprian arc (Figure 1). The North Anatolian fault is the seismically most active strike slip fault and it forms a transform plate boundary between the Anatolian and Eurasian plates in northern Turkey. The East Anatolian fault is also a transform fault and the seismically second most active fault in the region that runs along the tectonic boundary between the Anatolian and Arabian plates in eastern Turkey.

The Aegean-Cyprian arc is a convergent plate boundary, where the Nubian plate is subducting beneath the Anatolian plate. The East and North Anatolian faults

accommodate the southwestward motion of the Anatolian plate towards the Cyprian Arc (Jackson & McKenzie, 1984) as it is squeezed by continued collision with the Arabian and Eurasian plates.

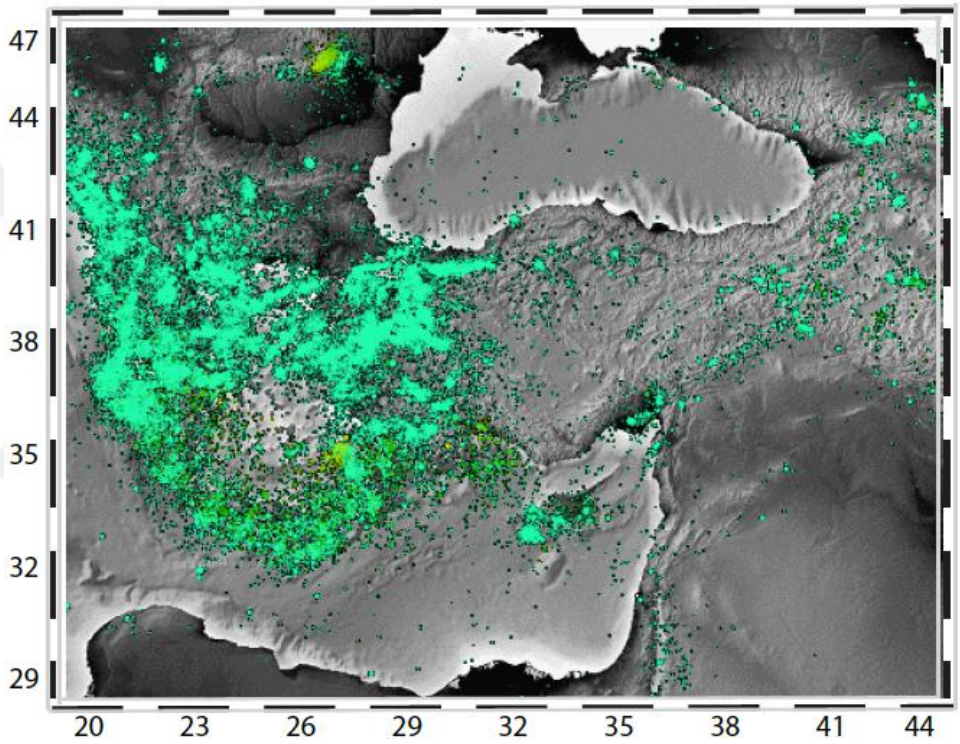

Figure 2.a. Seismicity of Anatolia from UNAVCO webpage (http://jules.unavco.org/Voyager/Earth).

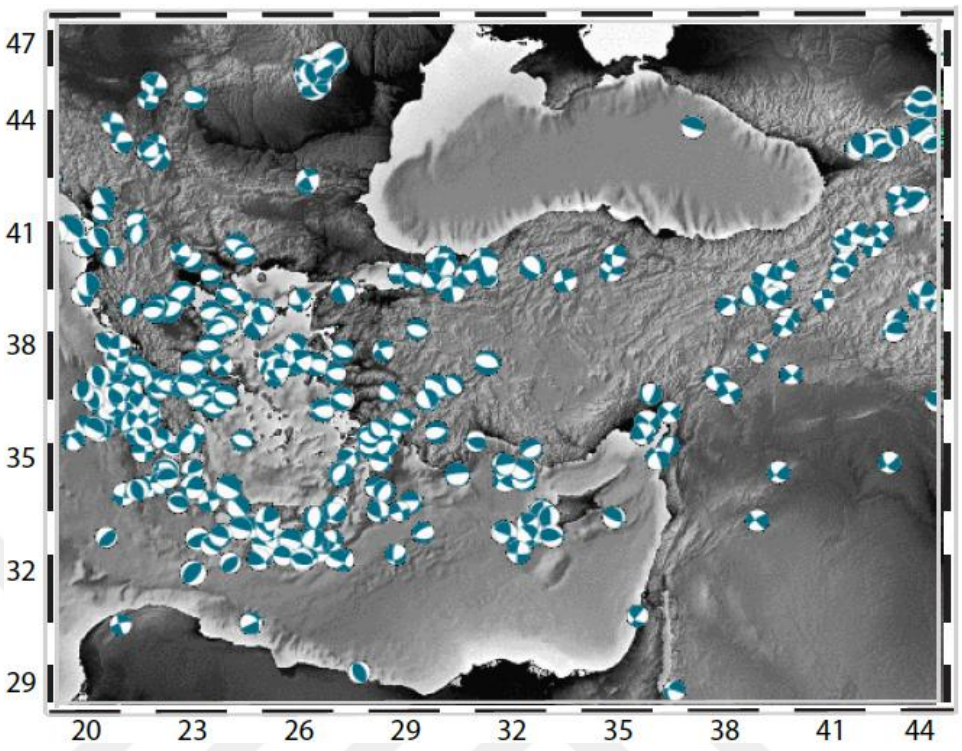

Figure 2.b. Focal mechanism (lower hemisphere projection) for earthquakes of the Anatolia from UNAVCO webpage (http://jules.unavco.org/Voyager/Earth).

Deformation in eastern Turkey is mostly driven by faulting during earthquake. Magnitude 7 and greater earthquakes are relatively common and occur often along the major faults; however, deformation in the Caucasus seems to happen aseismically (Jackson and McKenzie, 1988) (Figure 2.a and 2.b).

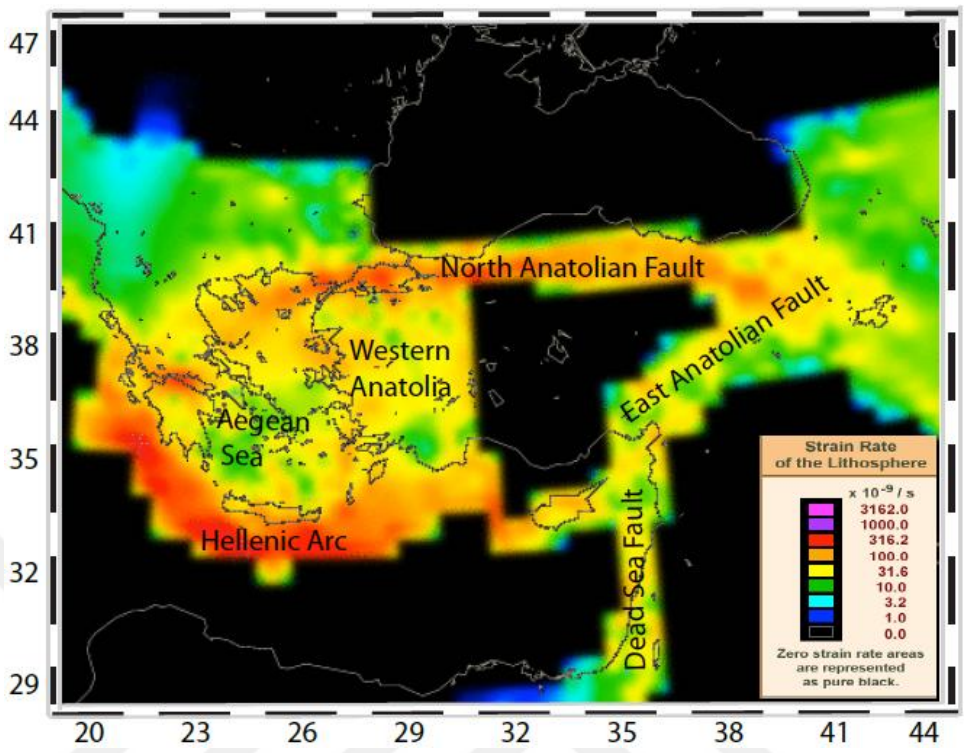

Figure 2.c. Strain rates of the litosphere of Anatolia and its surrounding region from UNAVCO webpage (http://jules.unavco.org/Voyager/Earth). Each color represents denseness of the strain rate area. Black represents zero strain area.

Figure 2.c indicates that strain rates are fairly high on plate boundaries and represented by mostly red and yellow. The Hellenic arc and North Anatolian Fault are highest strain areas in the Anatolia region. The East Anatolian and Dead Sea Faults are relatively less deformed than the Hellenic arc and North Anatolian Fault; however, deformation is still high.

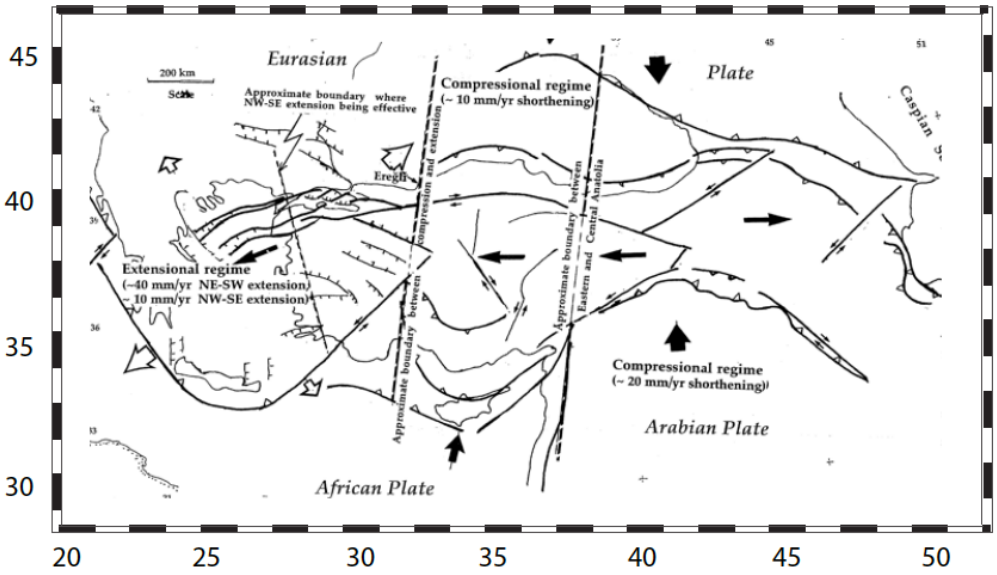

Figure 3. Neotectonic provinces of Anatolia showing the main tectonic features and related deformations. Data, is used here, mostly come from GPS measurement (Barka, 1997).

Sengor et al. (1985) argued that ongoing tectonics can be characterized by four apparent neotectonic provinces: (1) The East Anatolian contractional; (2) the North Anatolian, (3) the West Anatolian extensional; and (4) the Central Anatolian "ova" provinces (Figure 3).

The continental collision between the Eurasian and Arabian plates along the Bitlis-Zagros thrust belt initiated at late Miocene. The East Anatolian contractional province is located east of where the North and East Anatolian faults meet and represented by approximately north-south shortening and crustal thickening (Sengor et al., 1985; Philip et al., 1989). Dextral and sinistral strike slip faults parallel to the North and East Anatolian faults, north-south trending fissures that are associated with volcanoes are the main tectonic structures of the East Anatolian contractional province (Sengor et al., 1985; Philip et al., 1989; Bozkurt, 2001).

The North Anatolian province is located north of the North Anatolian fault and south of the Black Sea, and is described by east-west trending thrust faults (Sengor et al., 1985).

West-southwestward escape of the Anatolian plate along the North and East Anatolian faults leads to north-south extension of the west Anatolian (Figure 3). Roughly east-west trending graben and horsts are the main tectonic features of the West Anatolian Extensional province due to this north-south extension. However, the underlying cause of this extrusion is still under debate (Sengor et al., 1985; Bozkurt, 2001).

The Central Anatolian "ova" province is continental lithosphere that has experienced internal deformation along new or reactivated old structures (Figure 3). The region is represented by northeast-southwest shortening and northwest-southeast expansion. The strike slip faults of sinistral and dextral character and large terrestrial sediment-filled basins ("ovas") are the main structural elements of the Central Anatolian "ova" province (Sengor et al., 1985; Bozkurt, 2001).

B. Previous Block Model Results

Use of Global Positioning System (GPS) measurements to define deformations of the plates has increasingly been used in Earth Sciences. Analyses of the deformation of Anatolia Block have been conducted by McKenzie (1990), DeMets et al. (1990, 1994), McClusky et al. (2000), Westaway (2000), Barka and Reilingier (1997) and Reilinger et al. (2006).

Global plate tectonic models, defined by present-day plate motions, are derived from either studying earth quake slip vectors, ridge spreading rates and transform faults (eg., NUVEL-1A: DeMets et al., 1990, 1994) or GPS data. The NUVEL-1A global plate tectonic model suggested that the Arabian plate moves roughly northward at the rate of around 25 mm/yr (millimeter per year), averaged over nearly 3 m.y., relative to Eurasia. GPS measurements; on the other hand, indicate slower velocity for the Arabian plate at the rate of around 10 mm/yr (McClusky et al., 2000). McKenzie (1990) suggested that the northward motion of the Arabian plate, in consequence of continental collision with the Eurasia plate along the Zagros fold and thrust belt, is responsible for not only high seismic activity in eastern Turkey, but also westward escape of the Anatolian plate. Moreover, NUVEL-1A suggested that the African plate shows northward motion in a frame fixed to Eurasia at the rate of around 10 mm/yr, averaged over nearly 3 m.y. However, GPS measurements indicate much slower velocity as well as the African plate at a rate of around 5-6 mm/yr in a frame fixed to the Eurasia (McClusky et al., (2000). Velocity results of NUVEL-1A are considerably faster than that of GPS measurements (McClusky et al., 2000). Chu and Gordon (1998, 1999) estimated angular velocity for the African plate, which are consistent with GPS measurements (McClusky et al., 2000).

Calais et al. (2006) suggested that the discrepancy between their GPS estimate and Chu & Gordon's (1999) might be related to changes in the local plate kinematics.

Reilinger et al. (1997) claimed that it is the left-lateral motion along the Dead Sea transform fault that takes up, to a great extent, the differential motion between Africa and Arabia (about 15 mm/yr). They further suggest that the Aegean Sea is moving southward with respect to the Eurasia; therefore, the African plate subducts beneath the Aegean Sea along the Hellenic arc at a faster rate than the plate motion rate.

There is ongoing debate about westward extrusion of Aegean and western Anatolia. Many models have been suggested model to explain the Aegean and western Anatolia extrusion since the early 1970's. McKenize (1972, 1978) was one of the first to suggest that westward extrusion of the Aegean and western Anatolia is a result of the collision of the Africa-Eurasia plates, and this escape causes subduction of the African plate beneath the Aegean plate along the Hellenic trench. Westward motion of Anatolia is due to the gravitational energy related to the over-thickened continental crust within the collision zone. An alternate model in the mid-1980's suggested a similar hypothesis, that the extrusion of Anatolia is a consequence of the continental lithosphere at the southeast edge of Anatolia, where two plates collide with each other. However, continental lithosphere carries out the force reacting at the collision zone moving it westward (Sengor, et al., 1985). These two early models suggest that the starting of the extrusion in the Aegean and western Anatolia is a result of Arabia-Eurasia continental collision.

Since the late 1990's, new models have suggested that the primary force behind the extrusion of Anatolia is not because the Arabian plate at the south pushes against Anatolia. Conversely, it is because the Hellenic arc pulls Anatolia forward (Reilinger et

al., 2006). Global plate tectonic models (eg., GPS measurements: McClusky et al., 2000; Reilinger et al., 2006) show that the extrusion rates increase in the direction of Hellenic arc. Thus, they suggest that this rapid motion of Anatolia at the west requires forces being pulled rather than being pushed.

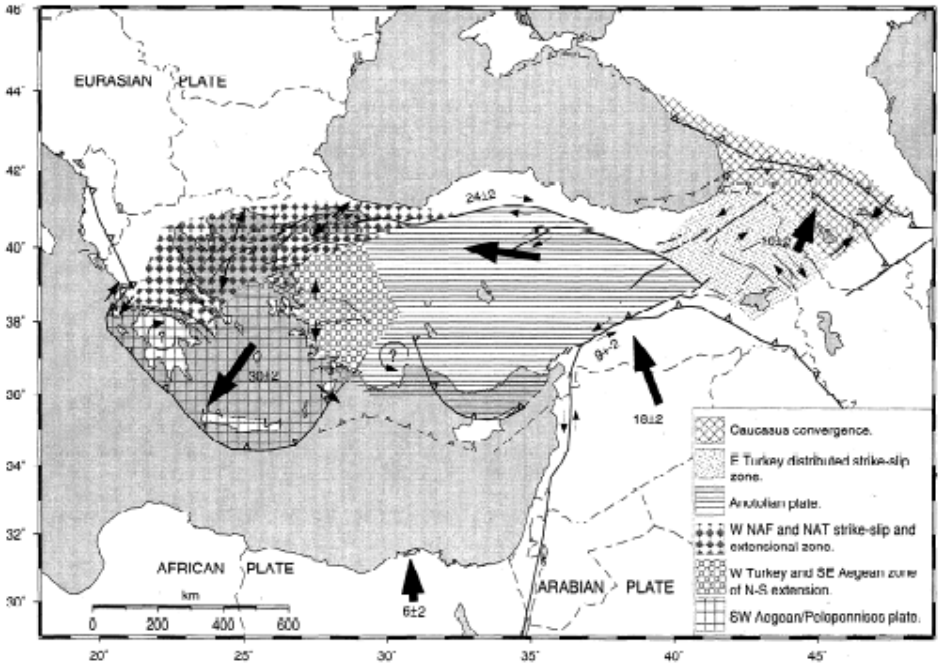

Figure 4. Schematic map of the principle results of McClusky et al. (2000). Hatching shows area of coherent motion and zone of disturbed deformation (see legend). Heavy arrows show generalized regional motion.

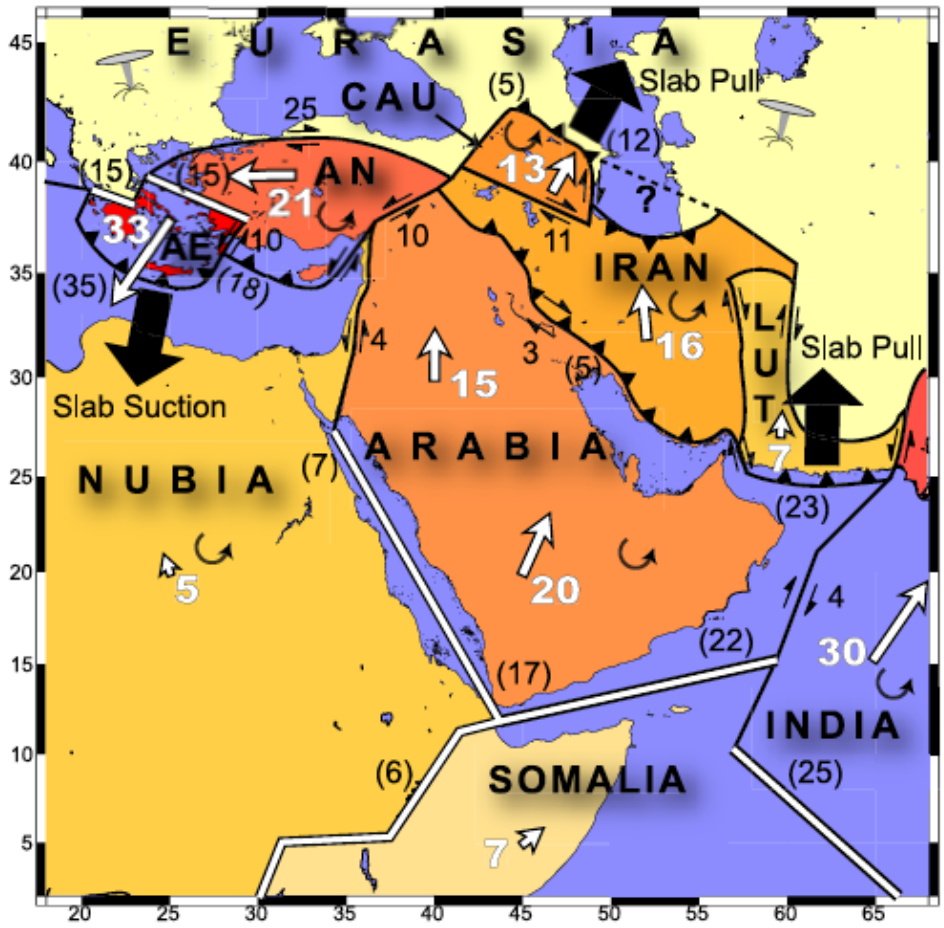

Figure 5. Schematic map of the Arabia-Africa-Eurasia zone of plate interaction illustrating the principal results of Reilinger et al. (2006). Abbreviations are Caucasus block (CAUC), Anatolia plate (AN) and Aegean plate (AE). Double lines, plain lines, and lines with triangles are extensional boundaries, strike-slip boundaries (paired arrows show direction of strike-slip motion), and are thrust faults respectively. Dark numbers are GPS-derived slip rates (mm/yr) on block-bounding faults (numbers in parentheses are dip slip and those without are strike slip). White arrows and matching numbers indicate GPS-derived plate velocities (mm/yr) fix to Eurasia. Curved arrows indicate sense of block rotation relative to Eurasia. Dark, heavy arrows indicate hypothesized forces related with active subduction.

The North Anatolian fault in the north and the East Anatolian fault in the south restrict the motion of Anatolia (McClusky et al., 2000). Jackson and McKenzie (1984, 1988) have presented an early approach to measure the relative motion of the western Anatolia-Aegean and the slip rate along the North Anatolian fault from seismological observations. Their predictions, nevertheless, are far from being certain since they estimate a 25-80 mm/yr slip rate on the North Anatolian fault but favor a rate of around

30 mm/yr within that range. Moreover, in their 30-110 mm/yr extension rate between the Aegean and Eurasia, they opt for a rate of around 60 mm/yr within that range. Geological slip rates for the North Anatolian fault are between 5 mm/yr and 20 mm/yr along different segments (Barka and Kadinsky-Cade, 1988, Kozaci et al., 2007). Dewey et al., (1986) indicated geologic slip rate for the East Anatolian fault left-lateral, average is about 4-7 mm/yr. GPS studies suggest higher slip rates than geological slip rate estimates for the North Anatolian faults and lower than rates based on seismological data. McClusky et al. (2000) estimated upper bounds on fault slip rates for the East and North Anatolian faults at about 9mm/yr and 24mm/yr, respectively (Figure 4). Reilinger et al. (1997) estimates are somewhat higher than those of McClusky et al. (2000) with slip rates of around 30 mm/yr for the North Anatolian fault and 15 mm/yr for the East Anatolian fault. However, Reilinger et al. (2006) (Figure 5), updating results presented by McClusky et al. (2000), estimated slip rates of the North and East Anatolian faults are in good agreement with GPS results McClusky et al. (2000).

C. Research Problem

Reilinger et al. (2006) showed that an elastic block model predicts a slip rate of about 25 mm/yr for the North Anatolian Fault (Figure 7), which is higher than the estimated geological rates of about 18 mm/yr. The objective of this study is to re-visit the block model study of Reilinger et al. (2006) and to examine this apparent slip rate discrepancy.

Until the late 1980's, geological methods such as offset of geomorphological markers were mainly used to determine historical slip rates along the faults. Since the mid 1990's, however, GPS has been widely used since it gives more accurate estimates of present-day slip rates by calculating strain accumulation at the crust.

In this thesis, I use the GPS derived velocity field of Anatolia including data from 1988 to 2005 by Reilinger et al. (2006). I use the extensive velocity data and published geologic slip rates to constrain an elastic block model. The elastic block model used in this study is a traditional block model that assumes no long-term deformation of the blocks. For simplicity, all faults are vertical and the words "plate" and "block" are synonymous in this model.

Along the North Anatolian fault, there is a discrepancy in slip rates between the two methods; the geologic slip-rate estimate for the North Anatolian fault is about 18 mm/yr while the geodetic estimate is around 25 mm/yr. To determine the best slip rates along the North Anatolian fault, I combined geologic and geodetic data into the model.
I then conducted elastic modeling to find the ranges of fault slip rates, which are consistent with the GPS velocities. This model allows us to change the weight of both the geodetic and geologic data to determine exactly how much discrepancy there is between geodetic and geologic data. This setup allows us to have both geodetic-only and joint inversion to estimate slip rates better.

Chapter 2 - Constraints and Modeling

A. Modeling and Data

The kinematic block modeling of interseismic surface motions has been used in different formats by several authors (e.g., McClusky et al. 2000; Westaway 2000; Barka and Reilingier 1997, 2006). The block modeling approach used here is described in Johnson and Fukuda (2010), however the method has been modified to assume long-term rigid block motions, unlike the deforming block model in Johnson and Fukuda (2010).

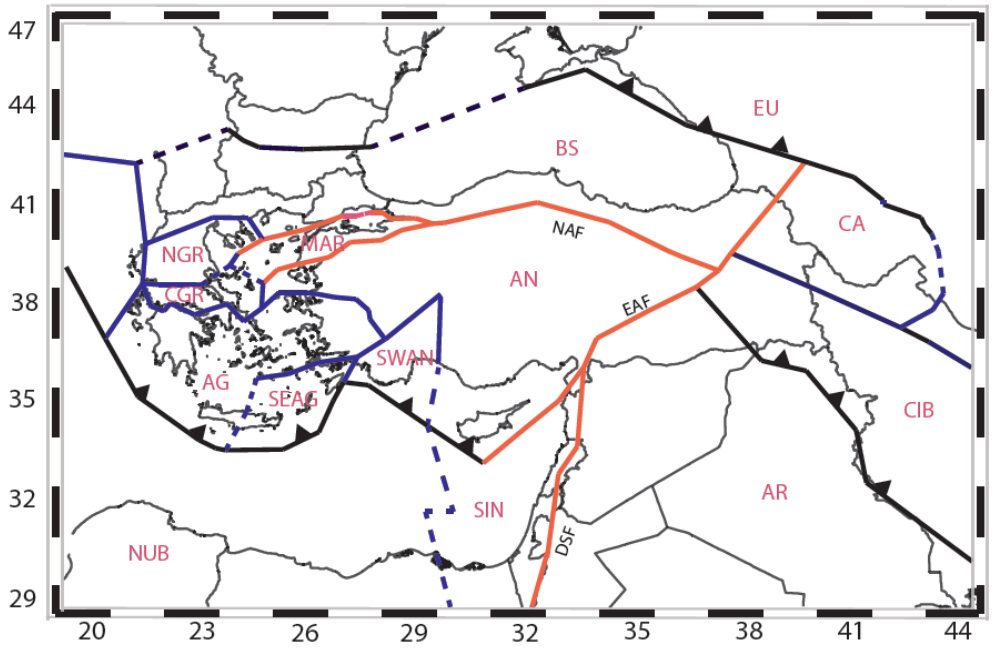

Figure 6. Map showing selected block model including of 14 blocks (or plates). Following Reilinger et al. (2006), block boundaries are defined from historic earthquakes, mapped faults and seismicity. Solid lines indicate well-defined boundaries whereas dash lines less well-defined boundaries. Black lines with triangles are thrust faults. Reddish lines are strike slip faults. Blue lines represent second major structures of the area. Abbreviations are Anatolian (AN), Eurasia (EU), Nubian (NU), Arabian (AR), Aegean (AG), Black Sea (BS), Central Iran Block (CIB), Caucasus (CA), Northern Greece (NGE), Marmara (MAR), Southwest Anatolian (SWAN), Central Greece (CGR), Sinai (SIN) and Southeast Aegean (SEAG).

Following Reilinger et al. (2006), block boundaries are defined from historic earthquakes, mapped faults and seismicity. Many of the major structures in Anatolia are well known except for a few submarine structures. Blocks and block boundaries for this model are defined on the basis of these previous studies. Locations of the structures in the model are not necessarily representing the exact location of real structures. Following Reilinger et al. (2006), I have adopted fourteen tectonic blocks: Anatolian, Eurasia, Nubian, Arabian, Aegean, Black Sea, Central Iran Block, Caucasus, Northern Greece, Marmara, Southwest Anatolian, Central Greece, Sinai and Southeast Aegean (Figure 6).

Segment Number	Latitude	Longtitude	Segment Name	Slip rate	Slip rate Uncertainties	References
1	41.1417	30.1526	GULF OF IZMIT (Western NAF)	10 mm/yr	-	Polonia et al. (2004)
2	40.4001	31.1001	MUDURNU (Western NAF)	11 mm/yr	5	Ikeda et al. (1991)
3	40.5011	31.1413	DUZCE-1 (Western NAF)	14 mm/yr	2.1	Pucci et al. (2008)
4	40.5004	31.1425	DUZCE-2 (Western NAF)	15.2 mm/yr	3.5	Pucci et al. (2008)
5	41.0776	34.5234	Ucoluk-Tosya (Central NAF)	18 mm/yr	3.5	Hubert-Ferrari et al. (2002)
6	42.0548	35.0001	TAHTA KOPRU-1 (Central NAF)	16.4 mm/yr	6.4	Kozaci et al. (2009)
7	42.0539	35.0025	TAHTA KOPRU-2 (Central NAF)	18.6 mm/yr	3.5	Kozaci et al. (2009)
8	39.2214	40.3938	DINARBEY (Eastern NAF)	20.4mm/yr	2.2	Zabci et al. (2010)

Table 1. Geologic slip rates from published papers. Segments numbers are used to show their location on the NAF (see Figure 11).

I combine GPS-derived velocities and geological slip rates (Table 1) to build kinematic block models of the Anatolian Plate and surrounding regions. In this thesis, I use the GPS derived velocity field of the Anatolian including data from 1988 to 2005 by

Reilinger et al. (2006). I use the extensive velocity data and published geologic slip rates to constrain an elastic block model.

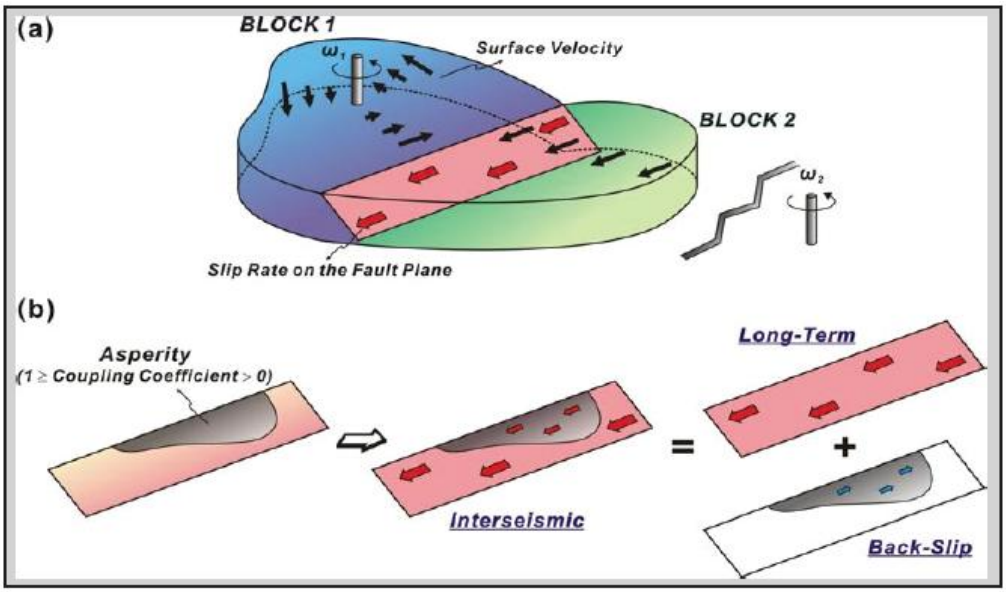

Figure 7. Idea of the 3D block modeling by Ching, et al. (2011). (a) Relationship between the Euler pole location and block movement. The black thick arrows show the orientation and magnitudes of the surface velocities in tectonic blocks. The pink plane (fault plane) is the interface between two blocks; w indicates rate of the rotation. Red arrows indicate the slip rates along the fault plane and the slip rates are derived from the velocity difference between two blocks. (b) Relationship between the long-term slip rate, back-clip rate (slip rate deficit) and interseismic slip rate. Red arrows indicate the slip rates along the fault plane, and the blue arrows are the back slip rates on the asperity.

The elastic block model used in this study is a traditional block model that assumes no long-term deformation of the blocks (Figure 7). For simplicity, all faults are vertical and the words “plate” and “block” are synonymous in this model and blocks are thought to be rigid.

Savage and Burford (1973) developed a 2D dislocation model to determine interseismic strain accumulation. This model has guided numerous researchers to determine velocities and strain rates using geodetic data. Here, using the back-slip model

approach of Savage and Burford (1973) and Savage (1983), the kinematically consistent block theory combines interseismic and long-term deformations. It is assumed that the interseismic velocity field is the sum of a long-term, rigid-body velocity field and an elastic, recoverable contribution from back-slip (locking) on faults.

The block model method was described by Johnson and Fukuda (2010), but the version used in this study is nearly identical to that of McCaffrey (2002) and Meade and Hager (2005). These are 3D elastic half space block models which are based on the screw dislocation model concept of Savage and Burford (1973). The 3D model assumes that there is no internal deformation at the blocks and they rotate around Euler pole without deforming (Figure 7).

In the inversion I use geodetic and geologic data to solve a least-squares problem for the Euler poles of rotation rate. The fault slip rates are simply a function of the Euler pole rotation rates. Relative weighting of the GPS and geologic slip rate data is varied to examine the sensitivity of the slip rate estimates to data constraints. Locking depth is related nonlinearly to observations. Therefore to estimate locking depth I conduct a grid search.

B. Methodology for estimating slip rates of the NAF

The purpose of this work is to constrain a model that is consistent with both geodetic and long-term geological data. Therefore, I use geologic slip rates as data in the geodetic inversion. Geologic slip rates for the North Anatolian Fault come from published papers and the location of the measurements, specified by longitude latitude coordinates, are used to assign to the appropriate location on the model fault. I conducted an extensive literature review to compile the geologic slip rate estimates listed in Table 1.

I present slip rate estimates for the both geodetic-only and joint inversions to examine the consistency geodetically derived slip rates with geologic slip rates along the North Anatolian Fault.

B. Locking Depth

Meade and Hager (2005) suggest that there is a relation between locking depth and fault slip rates. Shallower locking depth correlates with slower slip rate estimates; therefore, GPS velocities near locked fault have slower velocities (Reilinger et al., 2006).

Faults in the Reilinger et al. (2006) model are vertical and assigned a 15 km locking depth to correlate results against their previous resuls. The density of the GPS data near faults is not high enough to resolve detailed along-strike distribution of fault-locking depth (Reilinger et al., 2006), so I assumed a uniform locking depth for the entire region.

Meade and Hager (2005) suggested that an optimal locking depth can be selected from a plot of chi-square vs. locking depth. The best value for the locking depth is that which minimizes the chi-square; in other words, a chi-square tests for goodness of fit. I calculate normalized chi-square (sum of squared weighted residuals divided by number of observations) to estimate optimal locking depth along the NAF.

Chapter 3 - Results

The inversions provide both strike-slip and tensile fault (opening) slip rate estimates which are supported by plots of modeled, observed and residual velocities. The results are given in Table 2.

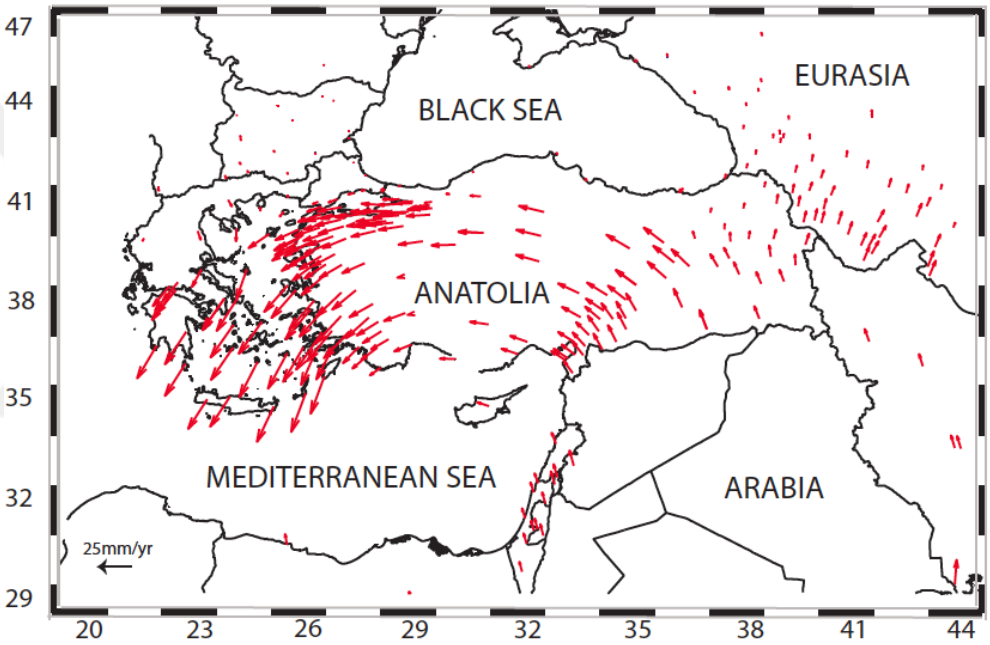

Figure 8. Map showing GPS model velocities with respect to Eurasia determined from geodetic-only inversion in this study.

On the basis of the GPS velocity field shown in Figure 8, Anatolia and Aegean blocks show counterclockwise motion with respect to the Eurasian plate. Moreover, the rate of this motion is increasing towards to the Hellenic arc and is almost twice as fast in the Aegean and in western Anatolia than in eastern Anatolia. These rates of motion increase in magnitude from about 18 mm/yr in eastern Anatolia to about 20 mm/yr in central Anatolia and about 25 mm/yr in western Anatolia and about 30 mm/yr in the

Aegean. The velocity field shown in Figure 8 also indicates that northeast Anatolian block shows northeastward motion with a rate of around 10 mm/yr.

The locking depth of the fault can be interpreted as the depth above which the majority of earthquakes occur. Hence, it is expected that locking depth variations are consistent with the focal depths of significant earthquakes (Meade and Hager, 2005).

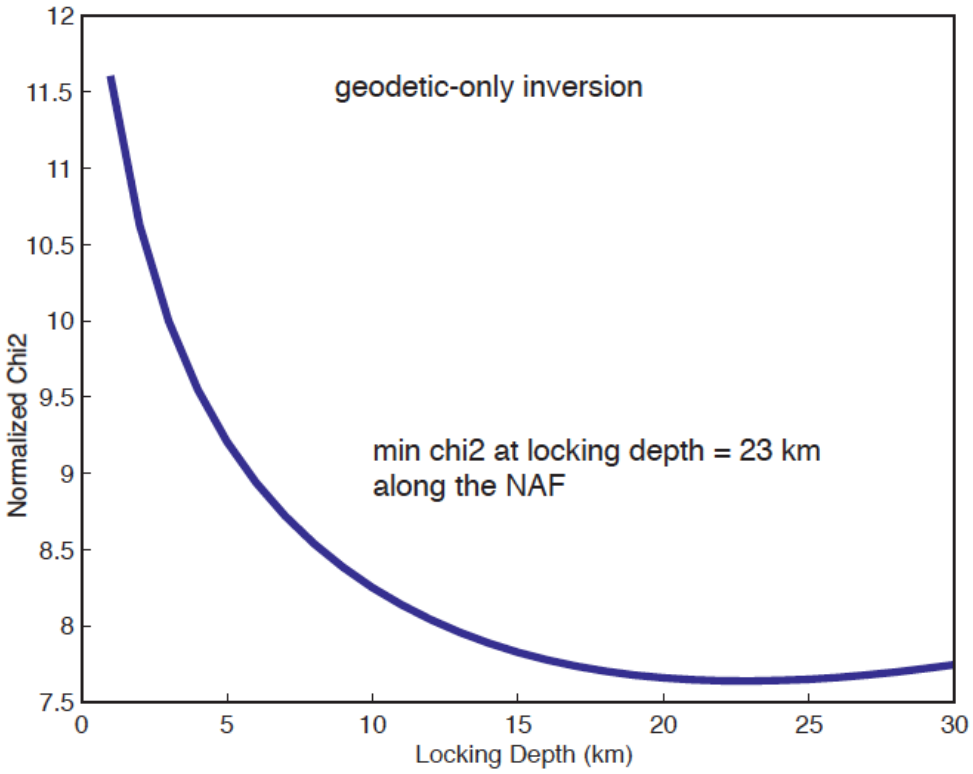

Figure 9. Normalized chi² determines how good the inversion fits the data, plotted versus locking depth for the North Anatolian fault. Velocity residuals are used to determine the chi². The best fit is for locking depths in the range 20– 25 km, preferably 23km in geodetic-only inversion.

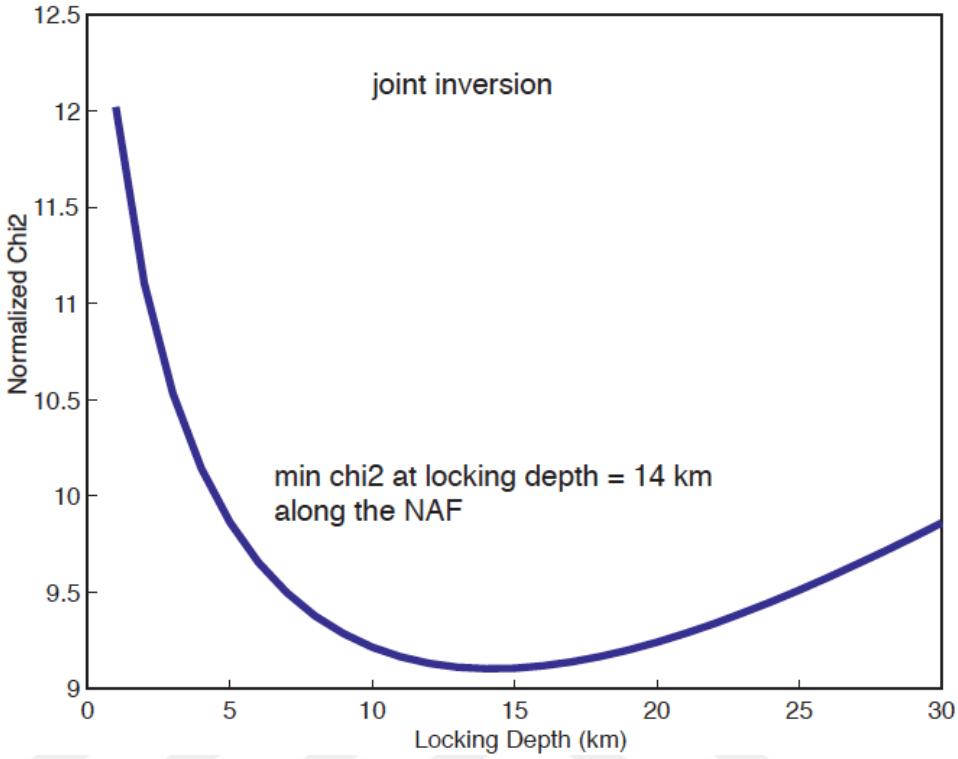

Figure 10. Normalized chi² determines how good the inversion fits the data, plotted versus locking depth for the North Anatolian fault. Velocity residuals are used to determine the chi². The best fit is for locking depths in the range 12– 16 km, preferably 14km in joint geodetic-geologic inversion.

I present a geodetic-only inversion and a joint inversion, to determine the best locking depth and slip rate variations of the North Anatolian Fault (NAF). The geodetic-only inversion implies a deeper locking depth along the NAF of around 20-25 km, preferably 23 km (Figure 9). The joint inversion, on the other hand, implies a shallower locking depth along the NAF of around 12-16 km, preferably 14 km (Figure 10).

This research shows that the locking depth of the NAF is in the range of 12- 16 or 20-25 km. Previous block model studies (eg., Reilinger et al., 2006) estimated locking depth variation in the range of 15-25 km along the NAF.

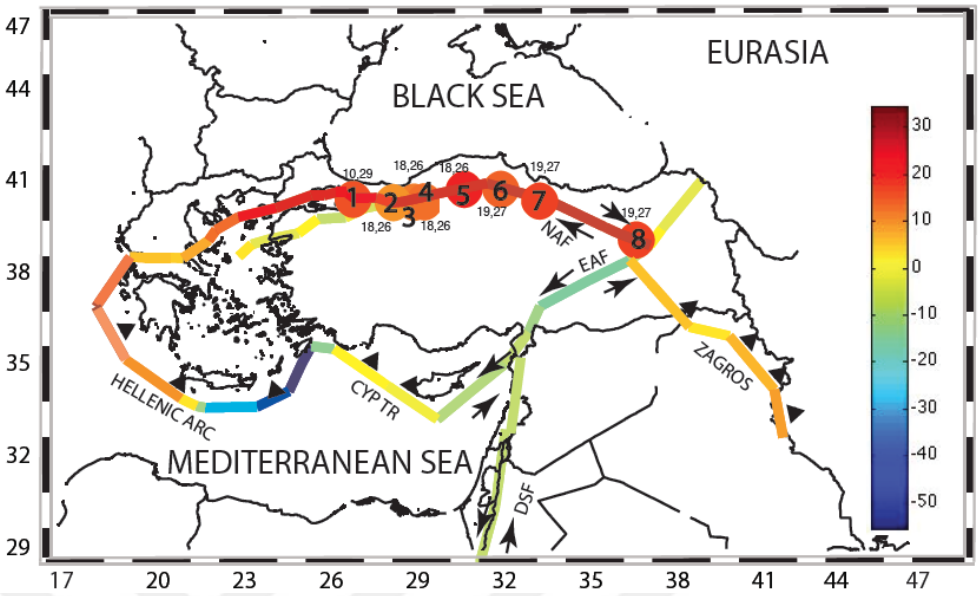

Figure 11. Slip rates along the North Anatolian Fault from both geodetic-only and joint inversion. Numbers represent joint geodetic-geologic and geodetic inversion slip rates respectively on each segment along the NAF. Colors of the structures represent slip rates along them. Right lateral strikes slip rates are positive numbers, whereas left lateral strike slip rates are negative numbers. Abbreviations are North Anatolian Fault (NAF), East Anatolian Fault (EAF), Dead Sea Fault (DSF) and Cyprus Trench (CYP TR). Numbers in the color balls indicate segments number to define slip rates on the NAF (See Table 1 and 2).

According to the geodetic-only inversion, the best slip rate estimation for the North Anatolian Fault (with optimal locking depth of 23 km) is 26-27 mm/yr (Figure 11), while the joint inversion (with optimal locking depth of 14 km) implies a lower strike slip rate along the NAF of 18-19 mm/yr (Figure 13). Combining the model results, I interpret that lower and upper bounds on fault slip rates for the NAF are 18-27 mm/yr, respectively (Figure 11).

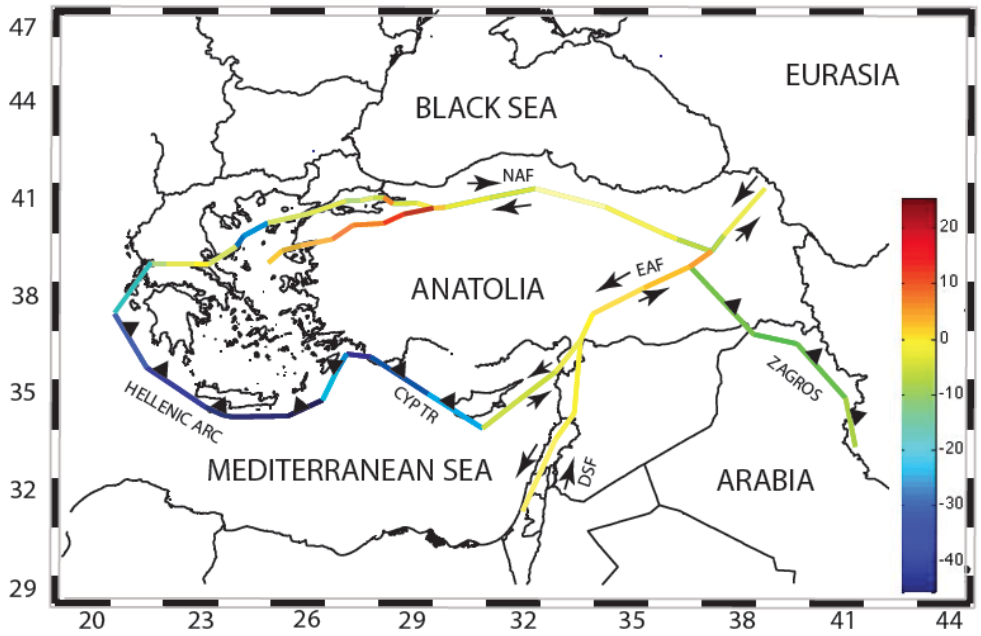

Figure 12. Map showing tensile rates along the major structures of Anatolia and it's surrounding area determined from geodetic-only inversion in this study. Abbreviations are North Anatolian Fault (NAF), East Anatolian Fault (EAF), Dead Sea Fault (DSF) and Cyprus Trench (CYP TR).

Segment Number	*Latitude*	*Longitude*	*Segment Name*	*Slip rate Uncer.*	*Joint Inversion Strike Slip Rates*	*Geodetic-only inversion Strike Slip Rates*
1	41.1417	30.1526	GULF OF IZMIT (Western NAF)	-	10.4532	29.4276
2	40.4001	31.1001	MUDURNU (Western NAF)	5	17.8051	25.5561
3	40.5011	31.1413	DUZCE-1 (Western NAF)	2.1	17.8507	25.6168
4	40.5004	31.1425	DUZCE-2 (Western NAF)	3.5	17.8563	25.6242
5	41.0776	34.5234	Ucoluk-Tosya (Central NAF)	3.5	18.0566	25.8874
6	42.0548	35.0001	TAHTA KOPRU-1 (Central NAF)	6.4	19.105	27.1283
7	42.0539	35.0025	TAHTA KOPRU-2 (Central NAF)	3.5	19.127	27.1265
8	39.2214	40.3938	DINARBEY (Eastern NAF)	2.2	19.0234	27.0255

Table 2. GPS derived Fault Slip Rates from Inversions. Segments numbers are used to show their location on the NAF (see Figure 13).

As previous researchers define it (Sengor et al., 1985; Barka, 1992), the NAF in northwest Anatolia is divided into two strands, the north and south strands (Figure 11). The northern strand is most likely to be the source of future large earthquakes in the region (e.g., Barka, 1999). The two large earthquakes, 1999 Izmit (Mw 7.4) and Duzce (Mw 7.1), occurred along the northern strand of the NAF (Meade et al., 2002). Slip rates along the northern strand of the NAF are almost four times faster than along the southern strand (Meade et al., 2002). My results also suggest that the rates along the northern strand of the NAF are significantly higher than along the southern strand. Tensile deformation along the NAF shown in Figure 12 indicates that the southern strand of the NAF in northwest Anatolia shows right lateral strike slip fault with a normal component.

Chapter 4 - Discussion

The GPS velocities with respect to Eurasia shown in Figure 8 quantifies the counterclockwise rotation of Anatolia and Aegean, which is increasing from east to west. Moreover, Figure 8 shows that there is a sudden change of the motion in eastern Anatolia east of the about 40^0 E and 38^0 N, where the Karliova triple junction is located (East of the Karliova triple junction and north of the Bitlis Suture zone in the Arabian-Anatolian plate collision zone). This area shows motion in the direction NNE causing shortening in the Caucasus (McClusky et al., 2000).

One of the biggest challenges of plate dynamics in the area is to understand what force mostly drives westward extrusion of Aegean and western Anatolia. Early models are mostly based on either Anatolia being pushed by the Arabian plate or over-thickened continental crust with high topography as a result of collision of the Africa-Eurasia plates drives westward extrusion of Aegean and western Anatolia. To sum up, these early models propose that the initiation of the extrusion in the Aegean and western Anatolia is a consequence of Arabia-Eurasia continental collision.

More recent models (e.g., McClusky et al., 2000; Reilinger et al., 2006); however, have principally focused on the idea that primary force behind the extrusion of Anatolia is not because the Arabian plate at the south pushes against Anatolia. In contrast, it is because the Hellenic arc pulls Anatolia forward since extrusion rates increase in the direction of Hellenic arc (Figure 8).

Early models require over-thickened crust, significant shortening within the eastern Anatolia and Caucasus, and the East Anatolian strike slip fault with a thrust component. However, more recent results (e.g., McClusky et al., 2000; Sengor et al.,

2003) have suggested slightly thickened crust and small amount of shortening within the eastern Anatolia and Caucasus. Furthermore, tensile deformation along the EAF shown in Figure 9 indicates that the EAF does not have thrust component whereas it might have small normal component. Based these observations, I suggest that primary force behind the extrusion of Anatolia is a slab pull along the Hellenic arc (Figure 8).

Two inversions, a geodetic-only inversion and a joint inversion, give the optimal locking depths is either 14 km or 23 km with in the range either 12-16 or 20-25 km respectively along the NAF. The geodetic-only inversion implies a deeper locking depth along the NAF of around 20-25 km, preferably 23 km (Figure 9). The joint inversion, on the other hand, implies a shallower locking depth along the NAF of around 12-16 km, preferably 14 km (Figure 10).

There are two possible interpretations for locking depth discrepancies. First is that geodetic-only inversion is a correct model representing the true seismogenic layer. The geodetic-only inversion result implying relatively deeper locking depth is consistent with some of the previous studies inferred from global positioning system (GPS) observations (e.g., Reilinger et al., 2006). Yolsal-Cevikbilen, et al. (2012), on the other hand, estimate that the depth of the lower limit of the seismogenic zone for north central Anatolia is about 15 km by applying local earthquake tomography. Besides, the brittle-ductile transition zone in this area is roughly defined with the range of 10-15 km based on averaged geothermal gradient (e.g., Brace and Kohlstedt, 1980; Sibson, 1982). Nevertheless, geodetically determined optimal locking depth of 23km is further down from the both brittle-ductile transition zone and the estimated depth of the lower limit of the seismogenic zone for the North Central Anatolia. A second interpretation would be

that the joint inversion results represent the true seismogenic layer. Ozalaybey et al. (2002) suggest the depths of the major earthquake and aftershocks of the 17 August 1999 Izmit earthquake, which occurred on the North Anatolian Fault are 13 km and 8-17 km, respectively.

It appears that the joint inversion provides better optimal locking depth estimate for the NAF than the geodetic-only inversion does; however, it is difficult to conclude this definitively. First of all, the optimal locking depth estimate along the NAF is uniform. Moreover, although estimates of the brittle-ductile transition from along the NAF are limited and the brittle-ductile transition depth seems to be spatially variable. Yolsal-Cevikbilen et al. (2012) estimate depth of the lower limit of the seismogenic zone is only central part of the NAF, which may not be representative of the entire NAF.

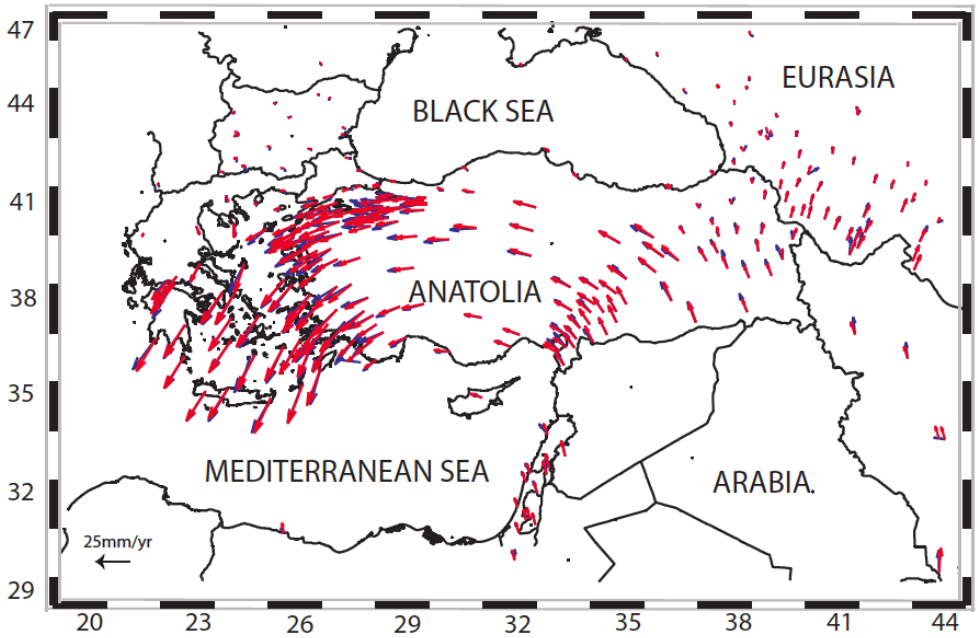

Figure 13. Map showing GPS model and data velocities with respect to Eurasia determined from geodetic-only inversion in this study. Red arrows indicate model, blue arrows indicate data.

The geodetic-only inversion and the joint inversion imply different strike slip rates along the NAF of around 26-27 mm/yr and 18-19 mm/yr respectively (Figure 11 and Table 1). There are four possible scenarios to explain this remarkable difference on slip rate estimates. The first and second scenarios would be that either geodetic slip rates or geologic slip rates are wrong. There are some limitations to estimate slip rates both on geodetic data and geologic rates. Insufficient GPS coverage along the fault zone (e.g., Reilinger et al., 2006) and large uncertainties on geologic estimates (e.g., Allen et al., 2004) would be examples for the limitations of the slip rate estimates. The third scenario would be that both of them are correct and the fault slip rates vary through time. Another possibility is that the GPS velocities vary with time because of flow in the mantle, which is neglected in these elastic block models.

The most apparent slip rate discrepancy between two models is on Gulf of Izmit along the NAF. The geodetic-only inversion predicts 29 mm/yr, while the joint inversion predicts about 10 mm/yr on Gulf of Izmit along the NAF.

Polonia et al. (2004) estimated the Holocene slip rate along the main segment of the NAF in the Gulf of Izmit to be roughly 10 mm/yr, which is smaller by factor of 2 and 3, than the geodetic motion estimate for the Anatolian plate with respect to Eurasia (e.g., Reilinger et al., 2006) and the geodetic-only inversion estimate from my work respectively. Polonia et al. (2004) suggested two hypotheses in order to clarify the discrepancy between the two independent estimates of slip rate. The first hypothesis is that deformation along this main segment of the NAF was not centered on a single fault, but it was diffuse and distributed between separate fault strands. The second hypothesis

is that geodetic estimates might represent a recent increase in slip rate; in this case the geodetic result does not represent the long-term geological motion.

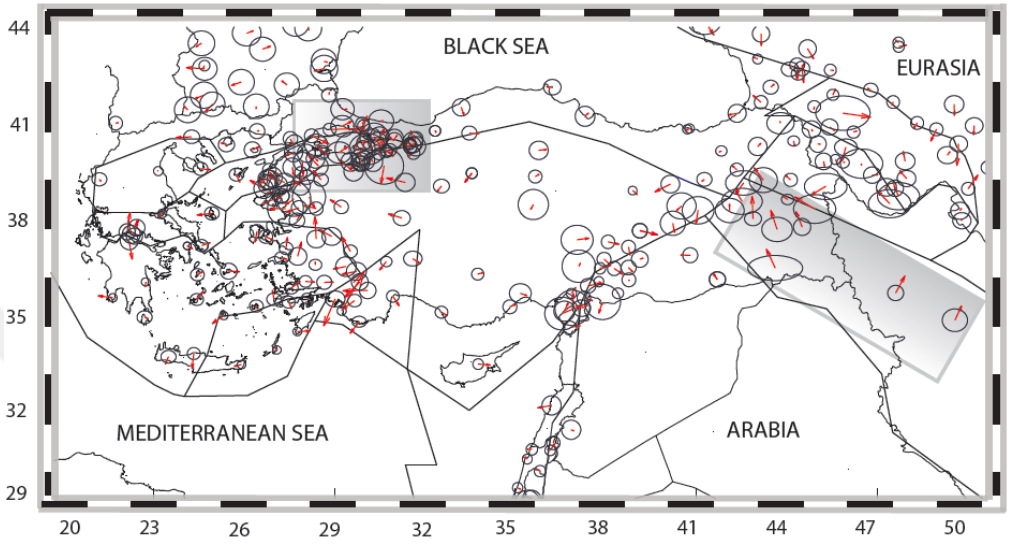

Figure 14. Map showing residual GPS velocities %95 confidence ellipses for a block model determined from geodetic-only inversion in this study. Marked (shadow) areas are related with insufficiency of model.

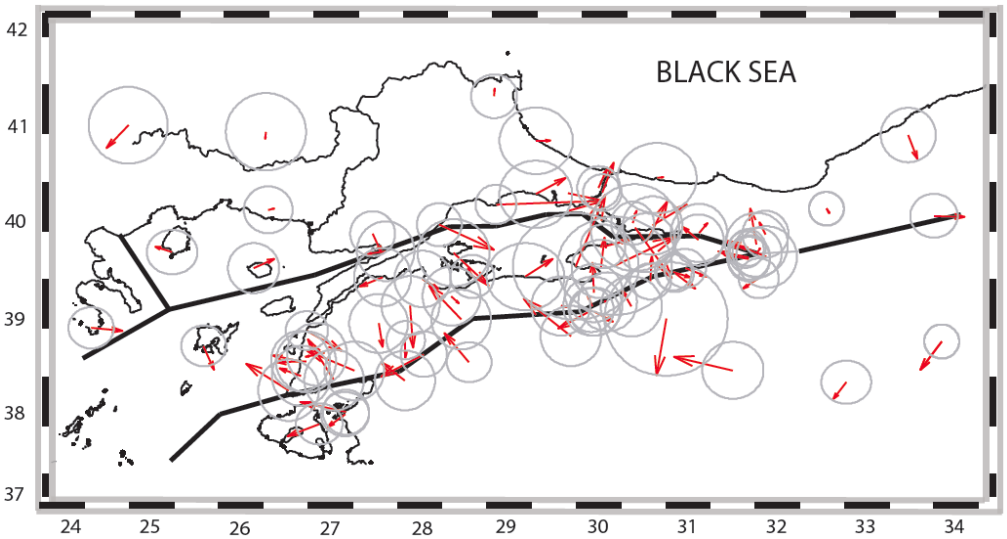

Figure 15. Map showing residual GPS velocities %95 confidence ellipses for a block model involving Marmara Blocks less constrained determined from geodetic-only inversion in this study.

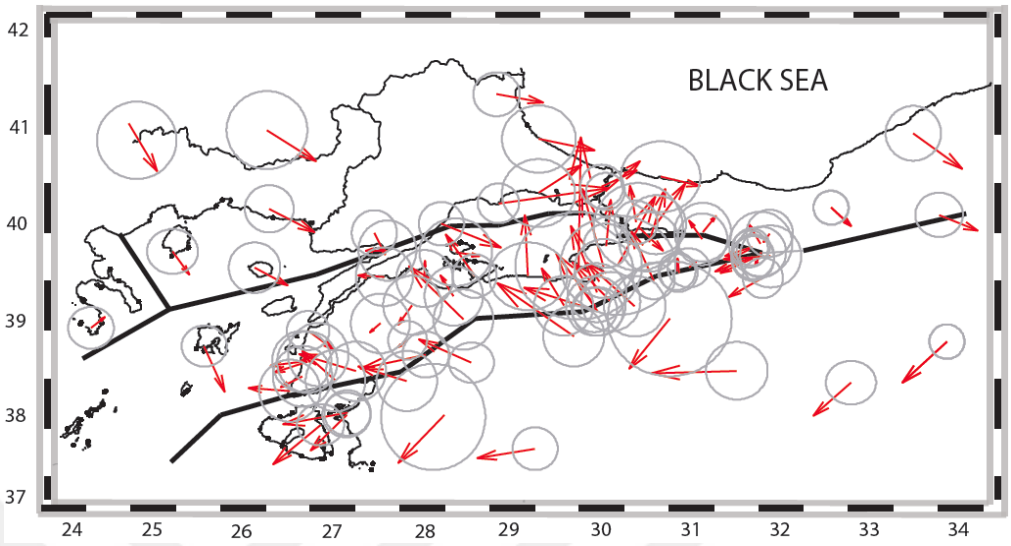

Figure 16. Map showing residual GPS velocities %95 confidence ellipses for a block model involving Marmara Blocks less constrained determined from joint inversion in this study.

This Holocene slip rate of the major segment of the NAF in the Gulf of Izmit may not represent the general behavior of the fault; however, the geodetic-only inversion slip rate is higher than previous studies inferred from global positioning system (GPS) observations (e.g., Meade et al., 2002). As shown in Figure 14, the residual velocities are largely within the error ellipses, however there are systematic misfits in the vicinity of the Gulf of Izmit NAF (the other location with systematic misfit is Eastern Anatolia). These systematic errors are a result of insufficiency of the model (eg., sudden change in deformation such as mantle flow, misplaced block boundaries, poor locking depth estimates). The systematic misfits near the Marmara sea occur in both the geodetic-only and the joint geodetic-geology inverions. The misfits might demonstrate that the predicted the predicted slip rate of 29 mm/yr in the geodetic-only inversion is excessively

high or the geodetic-geologic slip rate of 10 mm/yr is excessively slow. Systematic errors in Marmara might be also be associated with misplaced block boundaries since northern strand of the NAF (submarine fault) is trending along the Marmara Sea, which is not defined well.

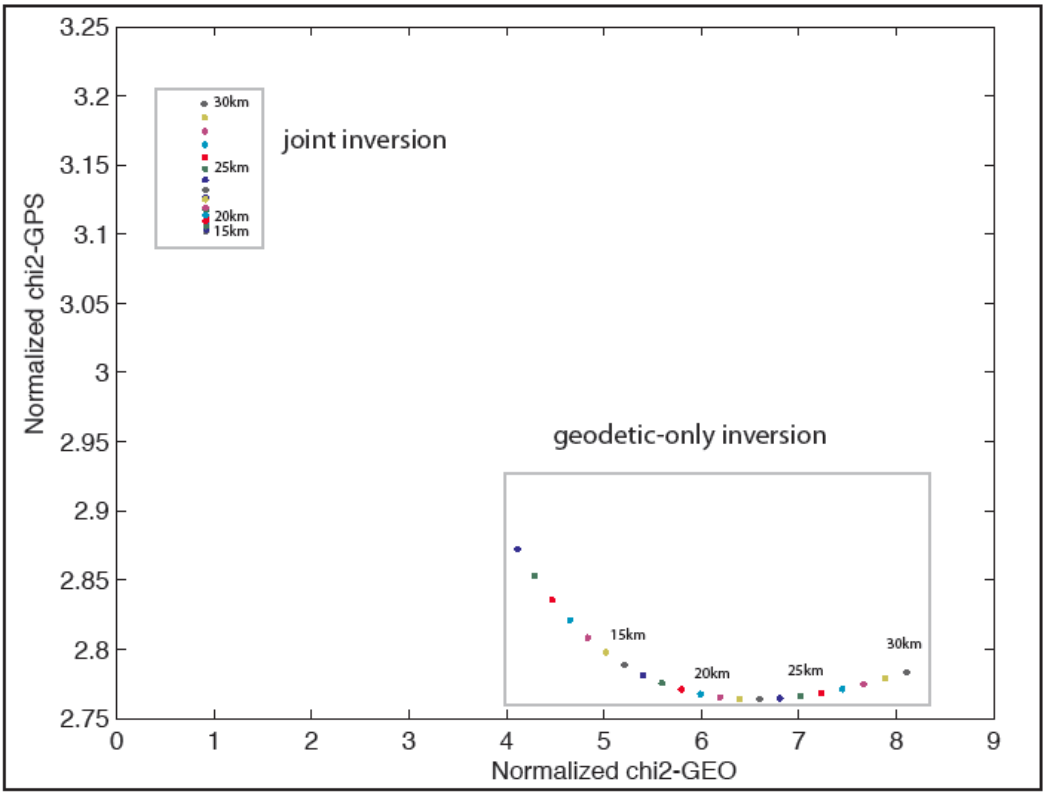

Figure 17. Comprasion plot of geodetic-only and joint inversion fit the GPS as a function of locking depth variations. Each point represents different locking depth variations from 10-30 km. Numbers represent locking depth of the point.

Figure 17 shows the plot of geodetic-only and joint inversion fit the GPS as a function of locking depth variations. Each point represents different locking depth variations from 10-30 km. A shallower locking depth variations for the joint inversion fits the GPS normalized chi^2 value of 3.1-3.2 (here normalized chi^2 is chi^2 divided by number

of observations); however, the GEO chi^2 value is not sensitive to locking depth variations because of the heavy weight placed on fitting the GEO data in the inversion. The geodetic-only inversion, on the other hand, fits the GPS data better than the joint inversion with a chi-square of around 2.8-2.9 compared to the joint inversion. However, the geodetic-only inversion does not provide acceptable agreement with the GEO data, with chi^2 fit of 4 to 8 for the GEO data, varying as a function of locking depth. As discussed before, the joint inversion gives locking depth and slip rates estimates that are in better agreement with independent observations than the geodetic-only inversion.

Chapter 5 - Conclusions

I use extensive velocity data from 1988-2005 by Reilinger et al. (2006) and published geologic slip rates to constrain an elastic block model of Anatolia. The elastic block model allows us to define plate motion and both strike-slip and tensile deformation rates along the major faults.

On the basis of the GPS velocity field shown in Figure 8, the Anatolia and Aegean blocks show counterclockwise motion with respect to the Eurasian plate. Additionally, the rate of this motion is increasing towards to the Hellenic arc and is almost twice as fast in the Aegean and in western Anatolia than in Eastern Anatolia.

A geodetic-only inversion and a joint inversion allow us to estimate the best locking depth and slip rate variations of the NAF. The geodetic-only inversion for the NAF gives approximately 26-27 mm/yr slip rate, implying a deeper locking depth of around 20-25 km, preferably 23 km (Figure 9). The joint inversion for the NAF, on the other hand, gives approximately 18-19 mm/yr slip rate, implying a shallower locking depth along the NAF of around 12-16 km, preferably 14 km (Figure 10).

The geodetic-only inversion matchs with the GPS data with a normalized chi-square value of 2.8-2.9, which is better than the joint inversion with a normalized chi-square value of 3.1-3.2 (Figure 17). Nevertheless, the slip rates of 18-19 mm/yr in the joint inversion are consistent with the geologic slip rates and the locking depths of 12-16 km are in good aggrement with the estimated depth of the lower limit of the seismogenic zone and depth of the major events along the NAF. This implies that joint inversion outcomes are compatible with more observational constraints than the geodetic-only inversion.

The last conclusion would be that south strand of the NAF shows right lateral strike slip fault with a normal component and is less active than the north strand of the NAF in northwest Anatolia.

References

Allen, M., J. Jackson, and R. Walker (2004), Late Cenozoic reorganization of the Arabia-Eurasia collision and the comparison of short-term and long-term deformation rates, Tectonics, 23, TC2008, doi:10.1029/ 2003TC001530.

Ambraseys N.N., C.F. Finkel (1991), Long-term seismicity of the Istanbul and of the Marmara Sea region, Terra Nova 3, 527 – 539.

Barka, A., (1992), The North Anatolian fault zone, Annales Tectonicae, VI suppl., 164-195.

Barka, A. (1999), The 17 August 1999 I˙zmit earthquake, Science, 285, no. 5435, 1858–1859.

Barka, A., and K. Kadinsky-Cade, (1988), Strike-slip fault geometry in Turkey and its influence on earthquake activity, Tectonics, 7, 663-684.

Bozkurt, E., and Mittwede S.K., (2001), Introduction to the Geology of Turkey—A Synthesis, International Geology Review, 43:7, 578-594

Brace, W. F., and D. L. Kohlstedt (1980), Limits on lithospheric stress imposed by laboratory experiments, J. Geophys. Res., 85, 6248 – 6252

Calais, E., DeMets C. & Nocquet, J.M. (2003), Evidence for a post-3.16 Ma change in Nubia- Eurasia plate motion. EPSL, doi:10.1016/S0012- 821X(03)00482-5.

Chu, D., and G. Gordon (1998), Current plate motions across the Red Sea, Geophys. J. Int., 135, 313– 328.

Chu, D., and G. Gordon (1999), Evidence for motion between Nubia and Somalia along the Southwest Indian ridge, Nature, 398, 64– 66.

Ching, K.E., R.J. Rau, K. M. Johnson, J.C. Lee, and J.C. Hu (2011), Present-day kinematics of active mountain building in Taiwan from GPS observations during 1995–2005, J. Geophys. Res., 116, B09405, doi:10.1029/2010JB008058.

Dewey, J.F., M.R. Hempton, W.S.F. Kidd, F. Saroglu, and A.M.C. Sengor, (1986), Shortening of continental lithosphere: The neotectonics of Eastern Anatolia- A young collision zone, in Collision Tectonics, edited by M.P. Coward and A.C. Ries, Geol. Soc. Spec. Publ. London, 19, 3-36.

DeMets, C., R.G. Gordon, D.F. Argus, and S. Stein (1990), Current plate motions, Geophys. J. Int., 101, 425-478.

DeMets, C., R.G. Gordon, D.F. Argus, and S. Stein (1994), Effects of recent revisions to the geomagnetic reversal time scale on estimates of current plate motions, Geophys Res. Lett., 21, 2191-2194.

Hubert-Ferrari, A., Armijo, R., King, G.C.P., Meyer, B. and Barka, A., (2002a), Morphology, displacement and slip rates along the North Anatolian Fault (Turkey). J. Geophys. Res., in press.

Ikeda, Y, Y. Suzuki, E. Herece, F. Saroglu, A.M. Isikara and Y. Honkura, (1991), Geological evidence for the last two faulting events on the North Anatolian fault zone in the Mudurnu Valley, western Turkey. Tectonophysics 193 (4), 335-345.

Jackson, J., and D.P. McKenzie, (1984), Active tectonics of the Alpine-Himalayan belt between western Turkey and Pakistan, Geophys. J.R. Astron. Soc., 77, 185-246.

Johnson, K. M., and J. Fukuda (2010), New methods for estimating the spatial distribution of locked asperities and stress-driven interseismic creep on faults with application to the San Francisco Bay Area, California, J. Geophys. Res., 115, B12408, doi: 10.1029/2010JB007703.

Kozaci, O., Dolan, J.F., Finkel, R., Hartleb, R., (2007), Late Holocene slip rate for the North Anatolian Fault, Turkey, from cosmogenic 36Cl geochronology: implications for the constancy of fault loading and strain release rates. Geology 35, 867–870.

Kozaci, O., J. F. Dolan, and R. C. Finkel (2009), A late Holocene slip rate for the central North Anatolian Fault, at Tahtakopru, Turkey, from cosmogenic 10 Be geochronology: Implications for fault loading and strain release rates, J. Geophys. Res., 114, B01405, doi: 10.1029/2008JB005760.

McClusky, S., et al. (2000), Global Positioning System constraints on plate kinematics and dynamics in the eastern Mediterranean and Caucasus, J. Geophys. Res., 105, 5695– 5719.

McKenzie, D. P. (1970), Plate tectonics of the Mediterranean region, Nature, 226, 239–243. Hodges, F. M. (2003).

McKenzie, D. P. (1970), Active tectonics of the Mediterranean region, Geophys. Jl, 18, 1– 32.

McKenzie, D.P. (1972), Active tectonics of the Mediterranean region. Geophys. J. R. Astron. Soc. 30, 109–185.

McKenzie, D. P. (1978), Active tectonics of the Alpine-Himalayan belt: The Aegean Sea and surrounding regions, Geophys. J. R. Astron. Soc., 55, 217– 254.

Meade, B.J., B.H. Hager, S.C. McClusky, R.E. Reilinger, S. Ergintav, O. Lenk, A. Barka, and H. Ozener (2002), Estimates of Seismic Potential in the Marmara Sea Region from Block Models of Secular Deformation Constrained by Global Positioning System Measurements, Bull. Seis. Soc. Am. 92, 208-215.

Meade, B. J., and B. H. Hager (2005), Block models of crustal motion in southern California constrained by GPS measurements, J. Geophys. Res., 110, B03403, doi:10.1029/2004JB003209.

Molnar, P. (1979). Earthquake recurrence intervals and plate tectonics. Bull. Seismol. Soc. Am. 69, 115 – 133.

Ozalaybey, S., M. Ergin, M. Aktar, C. Tapirdamaz, F. Bicmen, and A. Yoruk (2002), The 1999 Izmit earthquake sequence in Turkey: Seismological and tectonic aspects, Bull. Seismol. Soc. Am., 92, 376–386.

Polonia A.L. Gasperini, A. Amorosi, E. Bonatti, G. Bortoluzzi, N. Cagatay, L. Capotondi, M.-H. Cormier, N. Gorur, C. McHugh, L. Seeber (2004), EPSL, 227, 411–426

Pucci S, De Martini PM and Pantosti D, (2008), Preliminary slip rate estimates for the Duzce segment of the North Anatolian fault Zone from offset geomorphic markers. Geomorphology 97 (3-4): 538-554

Reilinger, R., et al. (1997), Global Positioning System measurements of present-day crustal movements in the Arabia-Africa-Eurasia plate collision zone, J. Geophys. Res., 102, 9983–9999.

Reilinger, R., et al. (2006), GPS constraints on continental deformation in the Africa-Arabia-Eurasia continental collision zone and implications for the dynamics of plate interactions, J. Geophys. Res., 111, B05411, doi:10.1029/2005JB004051.

Sengor, A. M. C., N. Gorur, and F. Saroglu (1985), Strike-slip faulting and related basin formation in zones of tectonic escape: Turkey as a case study, in Strike-Slip Faulting and Basin Formation, edited by K. T. Biddle and N. Christie-Blick, Spec. Publ. SEPM Soc. Sediment. Geol., 37, 227–264.

Sengor, A. M. C., S. Ozeren, T. Genc, and E. Zor (2003), East Anatolian high plateau as a mantle-supported, north-south shortened domal structure, Geophys. Res. Lett., 30(24), 8045, doi:10.1029/2003GL017858.

Sibson, R. H. (1982), Fault zone models, heat flow, and the depth distribution of earthquakes in the continental crust of the United States, Bull. Seismol. Soc. Am., 72(1), 151 – 163.

Yolsal-Cevikbilen, S., Biryol, C.B., Beck, S., Zandt, G., Taymaz, T., Adıyaman, H.E. and Ozacar, A.A. (2012), 3-D crustal structure along the North Anatolian Fault Zone in north-central Anatolia revealed by local earthquake tomography. Geophysical Journal International, 188 (3), 819-849.

C. Zabci, T. Sançar, H. S. Akyüz, N. G. Kiyak, Luminescence dating of offset terraces at the Elmali segment of the North Anatolian Fault (NE Turkey); Implications for long term geologic slip-rate", 2010, s. EGU2010-9212, EGU, Geophysical Research Abstracts, Vienna, 5/2/2010 - 5/7/2010.

http://jules.unavco.org/Voyager/Earth

VITA

Name : Mehmet Kokum

Date of Birth : June 4, 1985

Place of Birth : Elazig, Turkey

Education : B.S. Firat University, 2007
Geological Engineering

M.S. Indiana University, 2012
Geology and Geophysics